

# Dislocations in Si nanocrystals embedded in SiO<sub>2</sub>

Y Q Wang<sup>1,4</sup>, T Li<sup>1</sup>, W S Liang<sup>1</sup>, X F Duan<sup>2</sup> and G G Ross<sup>3</sup>

<sup>1</sup> The Cultivation Base for the State Key Laboratory, Qingdao University, No. 308, Ningxia Road, Qingdao 266071, People's Republic of China

<sup>2</sup> Beijing Laboratory of Electron Microscopy, Institute of Physics, Chinese Academy of Sciences, Beijing 100080, People's Republic of China

<sup>3</sup> INRS-EMT, 1650 Boulevard Lionel-Boulet, Varennes, QC, J3X 1S2, Canada

E-mail: [yqwang@qdu.edu.cn](mailto:yqwang@qdu.edu.cn)

Received 4 May 2009, in final form 30 May 2009

Published 14 July 2009

Online at [stacks.iop.org/Nano/20/315704](http://stacks.iop.org/Nano/20/315704)

## Abstract

Si nanocrystals (Si nc) were formed by the implantation of Si<sup>+</sup> into a SiO<sub>2</sub> film on (100) Si, followed by high-temperature annealing. High-resolution transmission electron microscopy has been used to investigate the dislocations in the Si nc produced by a high-dose (ion fluence of  $3 \times 10^{17} \text{ cm}^{-2}$ ) implantation. Three different kinds of dislocations, namely perfect, extended and mismatch dislocations, have been observed in some Si nc. The possible formation mechanism for these dislocations has been discussed. The dislocations in the Si nc are expected to have a great influence on the photoluminescence from Si nc embedded in SiO<sub>2</sub>.

## 1. Introduction

Si nanocrystals (Si nc) embedded in a SiO<sub>2</sub> matrix have attracted much interest as constituting a promising material for optoelectronics since the discovery of its photoluminescence at room temperature [1]. Some researchers [2, 3] ascribed the light emission to quantum confinement effects, while others [4, 5] thought that a defect center at the Si nc/SiO<sub>2</sub> interface plays an important role. Recent photoluminescence experiments under intense magnetic fields have shown that the emission from the Si nc of 1–3 nm embedded in an amorphous SiO<sub>2</sub> matrix is due to the formation of localized states at the Si nc/SiO<sub>2</sub> interface [6]. As we all know, the microstructure of materials determines their properties. So it is fundamental and important to give a comprehensive understanding of the microstructure of the Si nc and their surrounding matrix, especially the defects inside the Si nc or at the interface of Si nc/SiO<sub>2</sub>.

In our earlier papers [7–9], we have extensively investigated planar defects such as twinning and stacking faults (SFs) in the Si nc, and their influence on the photoluminescence intensity. Besides the planar defects, there are also linear defects (dislocations), defects of another type in crystals. Dislocations in bulk Si are known to cause states in the forbidden gap between the valence and conduction band,

which have a great influence on the photoluminescence from the bulk Si [10]. It is of interest to know how the influence of dislocations on Si nc differs from that on the bulk Si. Although a lot of reports focused on the investigation of dislocations in bulk Si, they have not been reported in Si nc up to now. In this paper, we report the observation of dislocations in the Si nc using high-resolution transmission electron microscopy (HRTEM). The formation mechanism of these dislocations is discussed. The dislocations might play an important role in the intensity decrease and redshift of the photoluminescence from the Si nc produced with a large excess of implanted Si (~50%) [7].

## 2. Experimental details

A 1 μm thick film of amorphous SiO<sub>2</sub> was obtained from [universitywafer.com](http://universitywafer.com). It was produced by thermal oxidation of (100) Si substrate at high temperature (~1100 °C under oxygen flow). The amorphous SiO<sub>2</sub> film was implanted at room temperature with 100 keV Si<sup>+</sup> ions to a high fluence of  $3 \times 10^{17} \text{ cm}^{-2}$  providing a local Si concentration in excess of ~50% at the mean implantation depth. The implantation was followed by high-temperature annealing at 1100 °C for 1 h under an atmosphere of nitrogen (N<sub>2</sub>) and a hydrogen (H<sub>2</sub>) passivation at 500 °C for 1 h in a forming gas of H<sub>2</sub> (5%) and N<sub>2</sub> (95%). The specimens for transmission electron

<sup>4</sup> Author to whom any correspondence should be addressed.

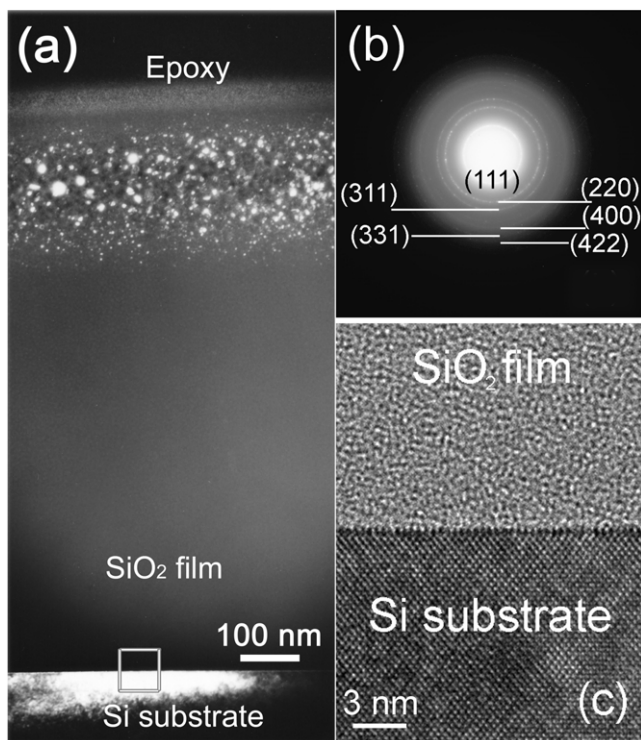


**Figure 1.** (a) Typical cross-sectional DF image of the specimen [11]; (b) SAED pattern taken from the Si nc embedded in SiO<sub>2</sub> [11]; (c) HRTEM image of the interface area (indicated by a rectangle in (a)) between the Si substrate and SiO<sub>2</sub> film.

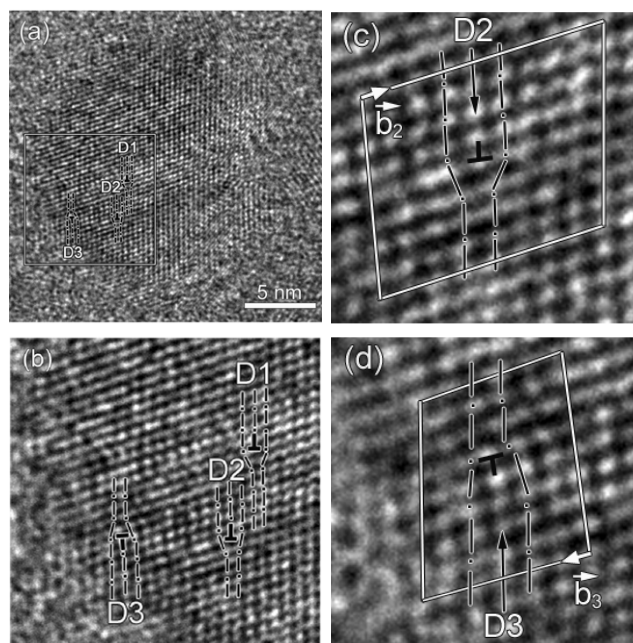
microscopy (TEM) examination were prepared in a cross-sectional orientation ([011] zone axis for the Si substrate) using conventional techniques of mechanical polishing, dimpling and ion thinning. The ion thinning was performed using a Gatan model 691 PIPS. Dark-field (DF) examination was carried out on a Philips CM30 microscope operating at 300 kV. HRTEM observations were performed using a JEOL JEM 2100F transmission electron microscope operating at 200 kV.

### 3. Results and discussion

Figure 1(a) shows a typical cross-sectional DF image of this specimen, and figure 1(b) is the selected-area electron diffraction (SAED) pattern taken from the Si nc embedded in the SiO<sub>2</sub> film, which can be indexed using the lattice parameters ( $a = 5.43 \text{ \AA}$ ) of Si [11]. From figure 1(a), it can be seen that the Si nc range from 2 to 22 nm in diameter, and the nanocrystals in the middle region of the implanted layer are larger than those near the free surface or the bottom of the layer. Before the DF and HRTEM examinations of the Si nc, the Si substrate was tilted to the [011] zone axis (figure 1(c)). From figure 1(c), it is shown that the interface between the Si substrate and the SiO<sub>2</sub> film is clean and flat.

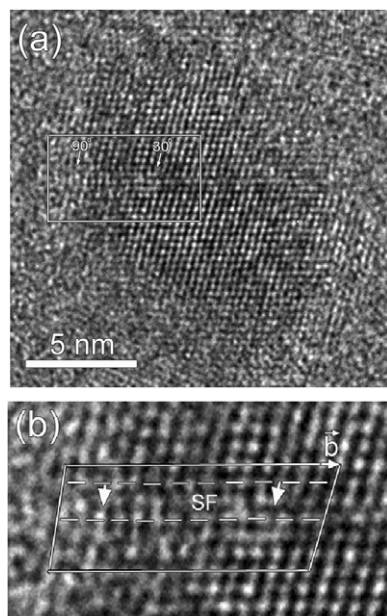
Extensive HRTEM observations show that there are three different kinds of dislocations inside the Si nc, namely, perfect, extended and mismatch dislocations. During the HRTEM observation, none of the Si nc exhibit structural fluctuation.

Figure 2(a) shows an example of a Si nanocrystal with three perfect dislocations, where the nanoparticle is oriented



**Figure 2.** (a) [011] zone axis HRTEM image of a typical Si nanoparticle with three perfect dislocations; (b) close-up of the three perfect dislocations (indicated by a rectangle in (a)) showing the extra half atomic planes; (c) Burgers circuit for D2; (d) Burgers circuit for D3.

along the [011] direction. The three dislocations are indicated by D1, D2 and D3 in figure 2(a), respectively. The extra half atomic plane, which is a characteristic of a perfect dislocation, is indicated by the dashed and dotted lines in figure 2(a). In order to show the extra half atomic planes more clearly, the enlarged HRTEM image of the three dislocations is shown in figure 2(b). For D1 and D2, the extra half atomic plane is inserted from above, while for D3, the extra half atomic plane is inserted from below, so D1 and D2 are regarded as positive perfect dislocations, and D3 is considered to be a negative perfect dislocation. To determine the Burgers vectors for D1, D2 and D3, Burgers circuits are drawn for D2 and D3 as shown in figures 2(c) and (d), respectively. From figures 2(c) and (d), we can clearly see that there is a gap between the starting and ending point of the Burgers circuit, which is indicated by an arrow. The Burgers vectors for D2 and D3 are determined to be  $\mathbf{b} = \frac{1}{2}\langle 110 \rangle$ , but they have opposite signs. The theoretical equilibrium configuration for the dislocations with the same sign is that one is located just above the other, while the equilibrium configuration for those with opposite signs is that the angle between the dislocation lines is 45°. The Burgers vectors for D2 and D3 have opposite signs; if they are on the same gliding plane, they will attract each other until annihilation occurs. Here D2 and D3 do not lie on the same gliding plane, so they will form an equilibrium configuration and the angle between the dislocation lines should be 45°. For D1 and D2, the Burgers vectors have the same sign but D1 does not locate just above D2 and cannot form an equilibrium configuration, so the interaction between them should be a repulsive force. The interaction between D1 and D3 is more complex because they are a little farther and separated by D2.



**Figure 3.** (a) [011] zone axis HRTEM image of a typical Si nanoparticle with an extended dislocation; (b) close-up of the extended dislocation showing two Shockley partials bounding a strip of SFs.

For the formation of the perfect dislocations, it could be due to the fact that the residual stresses arising from the volume contraction during the crystallization process of the Si nc could not be completely relieved [12].

Figure 3(a) shows a typical HRTEM image of a Si nanocrystal with an extended dislocation, where the nanoparticle is oriented along the [011] direction. It can be seen from figure 3(a) that two Shockley partial dislocations are connected by a strip of SFs. The two Shockley partials are indicated by two arrows and labeled as 30° and 90°, and the dislocation line directions are along [011]. The SFs have an intrinsic stacking fault characteristic with a displacement of  $\mathbf{R} = -\frac{1}{3}\langle 111 \rangle$  [8]. In order to demonstrate the configuration more clearly, the enlarged HRTEM image of the rectangle-enclosed region (in figure 3(a)) is shown in figure 3(b). The Burgers circuit enclosing the two Shockley partials (indicated by two arrows) is drawn in figure 3(b). From the Burgers circuit, it can be clearly seen that there is a gap between the starting and ending point, which is indicated by an arrow. The total Burgers vector is determined as  $\frac{1}{2}\langle 110 \rangle$ . In addition, the SFs' region is enclosed by the dashed lines in figure 3(b). In deformed bulk Si, the SFs and the dissociation of a 60° dislocation (Burgers vector  $\mathbf{b} = \frac{1}{2}\langle 110 \rangle$ ) into 30° and 90° partials (Burgers vector  $\mathbf{b} = \frac{1}{6}\langle 112 \rangle$ ) were observed using HRTEM at the beginning of the 1980s [13]. However, the dissociation has never been reported in the nanocrystalline Si. From our previous HRTEM observations [8], the SFs usually pass through the whole Si nanoparticle, and it is difficult to determine whether or not the SFs are formed due to the dissociation of a perfect dislocation. Here we can clearly see the boundary between the perfect and faulted lattice, so it could be interpreted by the dissociation of a perfect dislocation into

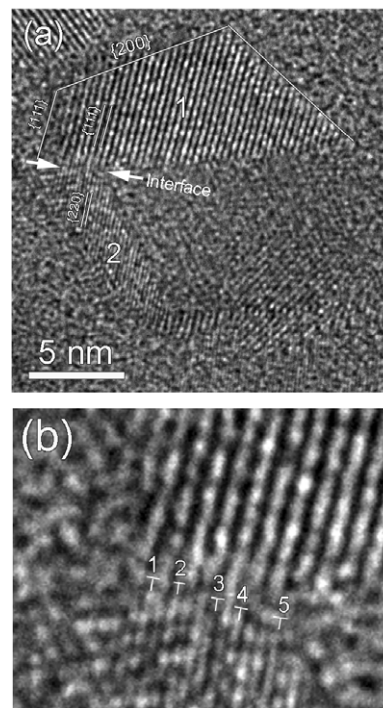


**Figure 4.** (a) HRTEM image of a coalesced Si nanoparticle with mismatch dislocations; (b) close-up of the mismatch dislocations.

two Shockley partials. A perfect dislocation might dissociate into two partials when it glides through the Si nc. The partial dislocations can be pinned at the Si nc/SiO<sub>2</sub> interface where some impurities are located [14].

Figure 4(a) shows an example of mismatch dislocations inside a coalesced nanocrystal, where the two Si nanoparticles have different crystal orientations. In nanocrystal 1, {111} planes are visible, while in nanocrystal 2, {220} planes are visible. In addition, nanocrystal 1 has clear facets, while nanocrystal 2 does not. The enlarged HRTEM image of the interface region is shown in figure 4(b), and the mismatch dislocations are indicated by T (labeled 1 to 5). The lattice spacing for the {111} plane is 3.14 Å, while the spacing for the {220} plane is 1.92 Å. Due to the different lattice spacings of the {111} and {220} planes, the mismatch dislocations are created to release the strain when the two nanoparticles join together during the annealing process. It is very clear that two small nanoparticles have coalesced into a bigger one because they have different crystal orientations. The coalescence behavior of Si nc [9] and gold nanoparticles [15] with same crystal orientations has been investigated before. The HRTEM image in figure 4(a) provides strong evidence for the coalescence of the Si nc during the growth process.

#### 4. Conclusions

In summary, three different kinds of dislocations, namely perfect, extended and mismatch dislocations, have been observed in the Si nc using HRTEM. The perfect dislocation could be caused by the residual stresses arising from the volume contraction during the crystallization of the Si nc. The



extended dislocations result from the dissociation of a perfect dislocation into two partials. The mismatch dislocations are caused by the coalescence of two particles with different crystal orientations. The dislocations in the Si nc are expected to have a great influence on the photoluminescence from the Si nc embedded in SiO<sub>2</sub> and could be responsible for the intensity decrease and redshift of the photoluminescence emission from the Si nc produced with large concentration of Si in excess.

### Acknowledgments

The authors would like to express their gratitude for the financial support from Qingdao University (Project No. 06300701), NanoQuébec and the Natural Science and Engineering Research Council of Canada (Project No. STPSC 356653-07).

### References

- [1] Averboukh B, Huber R, Cheah K W, Shen Y R, Qin G G, Ma Z C and Zong W H 2002 *J. Appl. Phys.* **92** 3564
- [2] Pinizzotto R F, Yang H, Perez J M and Coffey J L 1994 *J. Appl. Phys.* **75** 4486
- [3] Canham L T 1995 *Phys. Status Solidi b* **190** 9
- [4] Dinh L N, Chase L L, Balooch M, Siekhaus W J and Wooten F 1996 *Phys. Rev. B* **54** 5029
- [5] Shimizu-Iwayama T, Kurumado N, Hole D E and Townsend P D 1998 *J. Appl. Phys.* **83** 6018
- [6] Godefroo S, Hayne M, Jivanescu M, Stesmans A, Zacharias M, Lebedev O I, Van Tendeloo G and Moshchalkov V V 2008 *Nat. Nanotechnol.* **3** 174
- [7] Wang Y Q, Smirani R and Ross G G 2004 *Nano Lett.* **4** 2041
- [8] Wang Y Q, Smirani R and Ross G G 2005 *Appl. Phys. Lett.* **86** 221920
- [9] Wang Y Q, Smirani R, Ross G G and Schiettekatte F 2005 *Phys. Rev. B* **71** 161310R
- [10] Pizzini S, Binetti S, Le Donne A, Marzegalli A and Rabier J 2006 *Appl. Phys. Lett.* **88** 211910
- [11] Wang Y Q, Smirani R and Ross G G 2004 *Nanotechnology* **15** 1554
- [12] Miura H, Ohta H and Okamoto N 1992 *Appl. Phys. Lett.* **60** 2746
- [13] Olsen A and Spence J C H 1981 *Phil. Mag. A* **43** 945
- [14] Chen J Y, Eaglesham D J, Jacobson D C, Stolk P A, Benton J L and Poate J M 1996 *J. Appl. Phys.* **80** 2105
- [15] Wang Y Q, Liang W S and Geng C Y 2009 *Nanoscale Res. Lett.* **4** 684